Bull. Chem. Soc. Ethiop. **2025**, 39(7), 1381-1394.
DOI: https://dx.doi.org/10.4314/bcse.v39i7.11

ISSN 1011-3924
Printed in Ethiopia
Online ISSN 1726-801X

MESOMORPHIC AND THEMOCHMICAL BEHAVIOR OF A Cu(II)-CYCLAM IONIC LIQUID: A NOVEL APPROACH TO METALLOMESOGENS

Naima Sharmin[1], Md. Jahidul Islam[1], Md. Hafizul Islam[1], Moamen S. Refat[2*], Q. Mohsen[2] and Amnah Mohammed Alsuhaibani[3*]

[1]International University of Business Agriculture and Technology (IUBAT), Dhaka, Bangladesh
[2]Department of Chemistry, College of Science, Taif University, P.O. Box 11099, Taif 21944, Saudi Arabia
[3]Department of Sports Health, College of Sport Sciences & Physical Activity, Princess Nourah bint Abdulrahman University, PO Box 84428, Riyadh 11671, Saudi Arabia

(Received March 4, 2025; Revised March 16, 2025; Accepted March 18, 2025)

ABSTRACT. The metalomesogenic compounds exhibit captivating optical, magnetic, and electrical characteristics makes promising candidates for diverse applications in the fields of display devices, sensors, and molecular electronics. In this study, we focused on synthesizing the dark-purple powder of metallomesogen $[Cu(Cy)(L)_2](X)_2.2H_2O$, where Cy represents cyclam (1,4,8,11-tetraazacyclotetradecane), X is 4-BrC_6H_4COO-, and L is 4-Hexadecyloxypyridiene. The synthesis process involved four distinct steps. Differential scanning calorimetry (DSC) analysis revealed phase transitions at 42.3 °C (crystal-to-mesophase), 81.3 °C (mesophase-to-mesophase), and 111.7 °C (mesophase-to-isotropic liquid). Polarized optical microscopy (POM) confirmed the formation of characteristic optical textures upon cooling, indicative of a stable mesophase at 78.0 °C. The magnetic susceptibility measurements showed a magnetic moment of 1.7 Bohr magnetons, consistent with a mononuclear copper complex in a distorted octahedral geometry. These findings demonstrate the potential of this metallomesogen for applications in advanced display devices and sensors.

KEY WORDS: Metallomesogens, Ionic liquid, Cyclam, 4-Hexadecyloxypyridiene, Copper

INTRODUCTION

Liquid crystals are a unique state of matter that exhibit properties intermediate between those of liquids and solids. They possess the fluidity of liquids but also possess a degree of molecular order, like solids. This molecular arrangement allows them to respond to external stimuli like temperature, electric fields, and light, leading to a variety of optical and electronic properties [1-3]. Liquid crystals are widely used in displays, such as those found in televisions, computer monitors, and smartphones, as well as in optical devices like lenses and shutters [4, 5]. Metallomesogens are unique compounds that combine the characteristics of liquid crystals and metal complexes. These materials exhibit liquid-crystalline phases, like purely organic liquid crystals, due to the interactions between their anisotropic molecules. While mononuclear complexes have dominated metallomesogen research [6-8], introducing additional metal centers into these structures holds the potential for exciting new properties. For instance, binuclear carboxylates of divalent metal ions of transition series, such as copper(II), rhodium(II), ruthenium(II), molybdenum(II), palladium(II), and chromium(II), have been extensively studied and offer a promising avenue for exploring novel magnetic and electronic behaviors [9-14].

The metal-free macrocycles explored by Kang *et al.* exhibited columnar liquid crystal phases at room temperature, with the phase transition temperature varying depending on the chain length [15]. Introducing metal ions into these macrocycles is expected to maintain the columnar arrangement, leading to the formation of similar columnar phases in the corresponding metal

*Corresponding authors. E-mail: msrefat@yahoo.com

complexes [16]. This prediction is based on the structural similarity between the metal-free and metal-containing macrocycles, suggesting that the metal ions do not significantly disrupt the overall molecular packing and arrangement. When disk-like mesogens are arranged in columns; it gives rise to a suitable building block for anisotropic materials for exploiting those in electronic industries to manufacture conductors that are one dimensional [17], photoconductors [18], molecular fibers and wires [19, 20], LEDs [21] and photovoltaic (PV) cells [22]. A varieties of transition metals, such as Cu, Zn, Ni, Pt, Co, Pd, Cr, Pb, Mo have been incorporated with several macrocyclic tridentate [23], tetradentate [24-26] hexadentate [27] and octadentate [28] ligands to achieve hexagonal or rectangular columnar arrangements of discotic molecules. It is evident that the mesophases of the macrocyclic metallomesogens are more stable than that of their open chain counterpart [29]. In addition to stable mesophase; their self-assembly properties draw the researchers' attention for manufacturing commercial electronics specially [30]. However, there are not significant number of examples of metallomesogens where metals are fused in 1,4,8,11-tetraazacyclotetradecane (cyclam); reported in the literature.

In a recent report, Norbani and colleagues [31] synthesized a mesomorphic copper(II) complex with the ligand 1,4,8,11-tetraazacyclotetradecane (cyclam). The complex, denoted as $[Cu(cyclam)(L)_2](4\text{-}BrC_6H_4COO)_2$, incorporated 4-hexadecyloxypyridine (L) as a substituent. This complex exhibited mesomorphic behavior, indicating its ability to form liquid crystal phases. The presence of the cyclam ligand and the 4-hexadecyloxypyridine substitute contributed to the mesomorphic properties of this compound.

Metallomesogens, while offering unique properties, face limitations and challenges in their synthesis and applications. The incorporation of metal ions into liquid crystal structures can introduce complexities in the synthesis process, such as controlling the coordination environment of the metal and ensuring the formation of stable mesophases. Additionally, the choice of metal ions and ligands significantly influences the properties of the resulting metallomesogens, making it challenging to design materials with specific properties. Furthermore, the potential applications of metallomesogens are often limited by their thermal stability, solubility, and processibility.

This research aims to contribute to this field by focusing on the synthesis, thermochemical properties evaluation, and structural analysis of metallomesogens based on Cu(II) complexes with the cyclam ligand. By comprehensively studying these aspects, we aim to gain valuable insights into the factors influencing the properties and performance of these materials, paving the way for future advancements and applications. The findings of this research can contribute to the growing body of knowledge on metallomesogens and their potential applications in functional materials for optoelectronics, magnetic devices, and advanced display technologies. Furthermore, the enhanced thermal stability and unique magnetic properties of the synthesized complex open up possibilities for its use in high-performance sensors and molecular electronics.

EXPERIMENTAL

This study target to examine the synthesis and characterization of magnetic metallomesogen, $[Cu(Cy)(H_2O)_2]X_2.2H_2O$ where ligand (L) – 4-hexadecyl pyridiene ($4\text{-}CH_3(CH_2)_{15}OC_5H_4N$); cyclam (Cy) - 1,4,8,11-tetraazacyclotetradecane; X - $4\text{-}BrC_6H_4COO^-$. The metallomesogen incorporates a Cu(II) ion coordinated with cyclam, a macrocyclic ligand, and a functionalized benzoate derivative with fluorine at position 4. The synthesis involved a multi-step process starting with 4-fluoro benzoate, 1-bromohexadecane, and cyclam as precursors. By carefully selecting solvents and reaction conditions, we successfully obtained the target metallomesogen. Subsequent characterization studies aimed to elucidate the structural, magnetic, and liquid crystal properties of this compound using FTIR, NMR, XRD, UV, TGA, DSC and polarized optical micrograph (POM).

Materials

The following chemicals, sourced from Sigma-Aldrich and Merck, were utilized without additional purification: 4-hydroxypyridine (C_5H_5NO, 96% purity), 1-bromohexadecane ($CH_3(CH_2)_{15}Br$, 97% purity), potassium carbonate (K_2CO_3, 98% purity), 4-bromobenzoate ($C_7H_4BrO_2K$, 98% purity), potassium iodide (KI, 98.0% purity), potassium hydroxide (KOH, 97% purity), ethanol (C_2H_5OH, 98% purity), copper sulfate pentahydrate ($CuSO_4 \cdot 5H_2O$, 99.0% purity), N,N-dimethylformamide (DMF, $HCON(CH_3)_2$, 97.8% purity) and cyclam ($C_{10}H_{24}N_4$, 1,4,8,11-tetraazacyclotetradecane, 97% purity). The molecular structures of the precursor and intermediate compounds used in the synthesis of $Cu(Cy)(L)_{22} \cdot 2H_2O$ are depicted in Figure 1.

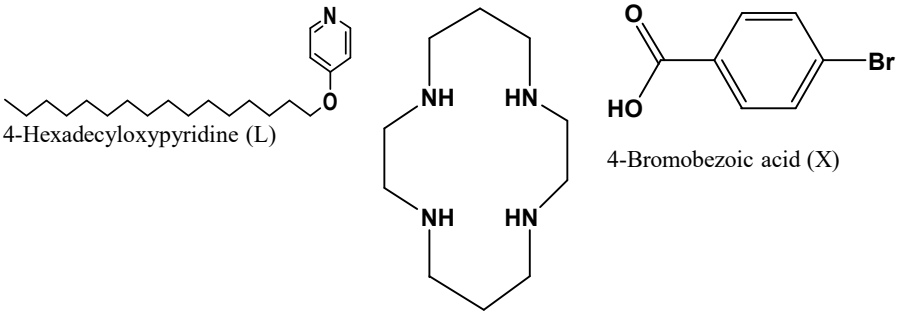

1,4,8,11-Tetraazacyclotetradecane
Cyclam (Cy)

Figure 1. Chemical formula of the corresponding ligand used for synthesis of copper metal associated liquid crystal $[Cu(Cy)(L)_2](X)_2.2H_2O$; where ligand (L) - 4-hexadecyl pyridiene ($4\text{-}CH_3(CH_2)_{15}OC_5H_4N$); cyclam (Cy) - 1,4,8,11-tetraazacyclotetradecane; X - $4\text{-}BrC_6H_4COO^-$.

Synthesis

The synthesis process involves a meticulous four-step procedure.

Ligand preparation. The 4-hexadecyloxypyridine ligand was synthesized through a nucleophilic substitution reaction between 4-hydroxypyridine and 1-bromohexadecane in the presence of potassium carbonate (K_2CO_3) and potassium iodide (KI) as a catalyst. The reaction was carried out in dimethylformamide (DMF) solvent under reflux conditions for 24 hours, yielding 88.8% of the desired product with high purity confirmed through ^{1}H-NMR analysis.

$$C_5H_5NO + CH_3(CH_2)_{15}Br + K_2CO_3 \xrightarrow[\text{Reflux}]{\text{DMF}} \text{4-Hexadecycloxypyridine} + KBr + CO_2$$

Copper(II) complex formation. The intermediate $[Cu_2(X)_4(EtOH)_2] \cdot 2H_2O$ was synthesized by reacting copper sulfate pentahydrate ($CuSO_4 \cdot 5H_2O$) with potassium 4-bromobenzoate ($4\text{-}BrC_6H_4COOK$) in ethanol at 60 °C for 30 min. This reaction yielded 61.9% of purple needle-shaped crystals, verified by elemental analysis and FTIR spectroscopy

$$2CuSO_4.5H_2O + 4\text{-}BrC_6H_4COOK \xrightarrow{EtOH,\ heat} [Cu_2(X)_4(EtOH)_2].2H_2O + 2K_2SO_4$$

Cyclam coordination. The complex $[Cu(Cy)(H_2O)_2](X)_2.2H_2O$ was obtained through a metathesis reaction by dissolving the copper precursor in a heated ethanolic suspension and adding cyclam. The reaction proceeded at 70 °C for 45 min, yielding the product with a purity of 57.7%, confirmed through UV-Vis spectroscopy and magnetic moment analysis.

$$[Cu_2(X)_4(EtOH)_2].2H_2O + Cy \xrightarrow{EtOH,\ heat} [Cu(Cy)(H_2O)_2(X)_2.\ 2H_2O$$

Final product formation. The final metallomesogen $[Cu(Cy)(L)_2](X)_2.2H_2O$ was synthesized by reacting $[Cu(Cy)(H_2O)_2]_2(X)_2 \cdot 2H_2O$ with 4-hexadecyloxypyridine in ethanol at 80 °C for 10 min. The resulting dark-purple powder was obtained with a yield of 68.5% and confirmed through FTIR and DSC analysis.

$$[Cu(Cy)(H_2O)_2(X)_2.\ 2H_2O + 2L \xrightarrow{EtOH,\ heat} [Cu(Cy)(L)_2(X)_2.2H2O + 2H_2O$$

Instrumental analyses

A Perkin-Elmer CHNS/O 2400 Series II elemental analyzer was used to perform elemental analysis on the samples. An AD-6 microbalance was used to weigh 1-2 mg of each sample. The samples were then encapsulated in small aluminum capsules (5 x 8 mm) and tightly folded to ensure a secure fit within the analyzer column. Subsequently, the encapsulated samples were introduced into analyzer and subjected to high temperatures, reaching a highest of 1000 °C, to facilitate the complete combustion and analysis of the elemental composition. Using a 400 MHz frequency spectrometer supplied by the JEOL firm, the sample's proton nuclear magnetic resonance (^{1}H-NMR) spectrum was obtained. A small quantity of the compound was made to dissolve in deuterated chloroform ($CDCl_3$) to serve as the solvent. $CDCl_3$ is a common solvent choice for NMR spectroscopy due to its deuterium nuclei, which do not interfere with the detection of proton signals. The FTIR spectra of the samples were collected using a Perkin-Elmer Spectrum 400 FT-IR/FTR/Pike 22107 Technologies Cladi ATARTM spectrometer in the spectral range of 4000-400 cm^{-1}. A little quantity of neat analyte was put in diamond anvil cell, ensuring direct contact between the detector and the sample surface. This configuration facilitated accurate measurement and analysis of the vibrational spectra. The magnetic properties of the synthesized complexes were investigated using the Gouy method to determine their magnetic susceptibility (χg) at 298 K, room temperature. A Sherwood Auto machine was employed to measure magnetic susceptibility, with distilled water serving as the calibrant. Those finely ground samples were put into a cylindrical shape tube having length of approximately 1.5 cm, as well their weight was recorded. The tube was then placed in the instrument to measure the χg value. The diamagnetic contribution (χdia) of each atom in the molecule was calculated using Pascal's constants [32], allowing for the determination of the molar susceptibility (χm). By subtracting the diamagnetic contribution from the molar susceptibility, the corrected molar susceptibility ($\chi Mcorr$) was obtained. Finally, the magnetic moment (μ_{eff}) was calculated using the formula $\mu_{eff} = 2.828(\chi M_{corr}T)^{½}$, where T is the temperature in Kelvin. This analysis provides valuable insights into the magnetic behavior of the synthesized complexes. Using a UV-Visible-NIR spectrophotometer, the sample's absorbance was measured between 300 and 2000 nm in wavelength. The sample was prepared by dissolving it in a suitable solvent and transferring the solution to a cuvette made of quartz. The spectrum was tallied relative to the used solvent, ensuring that any absorbance observed was due to the sample itself. This technique allows for the identification and quantification of specific chemical species based on their characteristic absorption patterns within the specified wavelength range. The photomicrographs of the

synthesized complexes were obtained using the olympus polarizing optical microscope which was equipped with a Linkam THMS 600 hot stage and Mettler Toledo FP90 central processor. Prior to analysis, the samples were nicely ground as well dried by oven setting temperature at 60 °C for overnight to remove any residual moisture. Heating/cooling scale were systematically changed within 2 - 10 °C/min to investigate their influence on the observed phenomena. The magnification used for imaging was 50x, providing a detailed view of the sample morphology and any temperature-dependent changes. To perform thermogravimetric analysis (TGA), a Perkin-Elmer 4000 TG/DTA Thermal System was used. Samples (2-5 mg) were placed in a ceramic pan and heated from 35°C to 900°C at a rate of 20°C/min under a nitrogen atmosphere (10 mL/min). The analysis monitored weight loss as a function of temperature, providing information about the thermal stability and decomposition behavior of the samples. DSC was conducted using both a Perkin-Elmer DSC6 and METTLER TOLEDO DSC822 and to analyze the thermal properties of the sample. Approximately 2-8 mg of the sample was accurately weighed and placed in an aluminum crucible. The crucible was then inserted into the DSC heating stage and subjected to multiple heating and cooling cycles within a temperature range of 25-300 °C, with a scan rate of 10 °C/min. The analysis was performed under a nitrogen atmosphere at a flow rate of 10 mL/min to minimize oxidation and other environmental factors that could affect the results.

RESULTS AND DISCUSSION

The target of this investigation was to synthesize and evaluate magnetic and metallomesogens properties with the formula $[Cu(Cy)(L)_2](X)_2.2H_2O$. The ligand L, 4-hexadecyloxy pyridine, is a long-chain alkyloxy pyridine derivative, while cyclam (Cy) is a macrocyclic tetraamine ligand. The counterion X is 4-bromobenzoate. The synthesized compounds were then evaluated for their liquid crystal properties. This investigation aimed to explore the potential of these metallomesogens as functional materials with unique magnetic and liquid crystalline characteristics.

Synthesis and characterization of hexadecyloxypyridine-4 ligand (L)

4-Hexadecyloxypyridine (L) was successfully synthesized through a nucleophilic substitution reaction between hydroxypyridine-4 and bromohexadecane-1 in presence of a base (K_2CO_3) and a catalyst (KI) in dimethylformamide (DMF). The reaction yielded a pale brown powder with an 88.8% yield, indicating good efficiency.

The structure of L was confirmed by ^{1}H-NMR spectroscopy. The aromatic protons exhibited a multiplet at 7.26, as well as a quartet at 6.39 in ppm, respectively. The methylene protons adjacent to the oxygen atom appeared as a triplet peak at 3.75 in ppm. The remaining -CH_2- protons within the alkyl chain resonated as a multiplet at 1.25 ppm. Finally, the terminal methyl protons were observed as a triplet at 0.88 ppm. These spectral assignments are consistent with the expected structure of 4-hexadecyloxypyridine.

The FTIR spectra of the ligand 4-hexadecyloxypyridine (L), the intermediate complex $Cu(Cy)(H_2O)_2](X)_2.2H_2O$ and the final metallomesogen $[Cu(Cy)(L)_2](X)_2.2H_2O$ were analyzed to confirm their structures and coordination environments (Figure 2). Key vibrational bands provide insights into the functional groups and bonding in these compounds.

The FTIR spectrum of 4-hexadecyloxypyridine (L) shows characteristic bands at 2919 cm^{-1} and 2851 cm^{-1}, corresponding to asymmetric and symmetric CH_2 stretching vibrations, typical of long alkyl chains. The C=N stretching vibration at 1638 cm^{-1} confirms the pyridine ring, while the C-O stretching vibration at 1188 cm^{-1} indicates the ether linkage. These bands confirm the successful synthesis of the ligand.

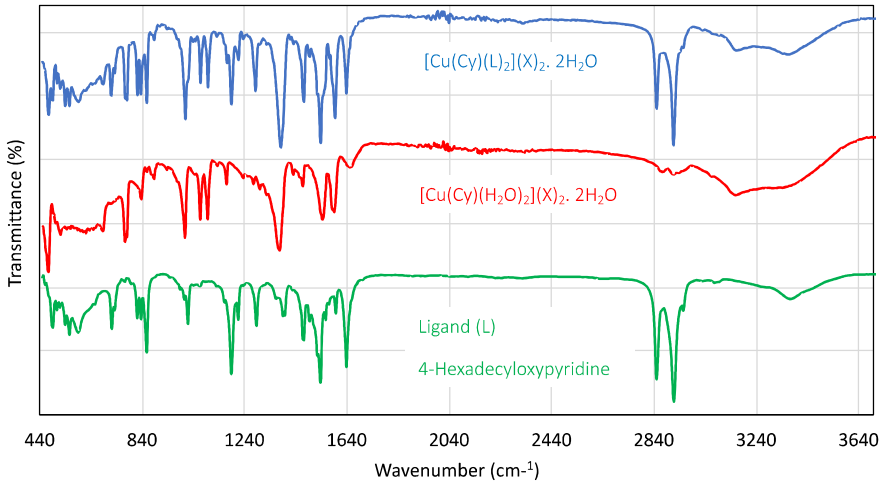

Figure 2. Data assignments by FTIR of ligand (L), $[Cu(Cy)(H_2O)_2](X)_2.2H_2O$ and $[Cu(Cy)(L)_2](X)_2.2H_2O$; where ligand (L) - 4-hexadecyl pyridine (4-$CH_3(CH_2)_{15}OC_5H_4N$); cyclam (Cy) - 1,4,8,11-tetraazacyclotetradecane; X - 4-$BrC_6H_4COO^-$.

The spectrum of $Cu(Cy)(H_2O)_2](X)_2.2H_2O$ reveals a broad band at 3373 cm^{-1} due to O-H stretching from water molecules, and a band at 3191 cm^{-1} from N-H stretching in the cyclam ligand. The carboxylate group shows asymmetric and symmetric stretching vibrations at 1549 cm^{-1} and 1379 cm^{-1}, respectively, with a $\Delta\nu$ value of 170 cm^{-1}, indicating non-coordinated carboxylate ions. A band at 1097 cm^{-1} corresponds to C-N stretching in cyclam, confirming its coordination to Cu(II).

The spectrum of $[Cu(Cy)(L)_2](X)_2.2H_2O$ exhibits a broad O-H stretching band at 3387 cm^{-1} and an N-H stretching band at 3182 cm^{-1}. The carboxylate vibrations at 1638 cm^{-1} and 1472 cm^{-1} ($\Delta\nu$ = 166 cm^{-1}) suggest non-coordinated carboxylate groups. The C=N stretching vibration at 1638 cm^{-1} and the C-O stretching vibration at 1189 cm^{-1} confirm the presence of the ligand L in the complex. The C-N stretching band at 1097 cm^{-1} further supports cyclam coordination. The key difference between the intermediate and final complex is the appearance of the C=N stretching vibration at 1638 cm^{-1} in the final metallomesogen, confirming the coordination of L. The reduced intensity of the O-H stretching band in the final complex suggests partial displacement of water molecules upon ligand coordination.

Table 1. Data assignments by FTIR of Ligand (L), $[Cu(Cy)(H_2O)_2](X)_2.2H_2O$ and $[Cu(Cy)(L)_2](X)_2.2H_2O$; where ligand (L) – 4-hexadecyloxy pyridine (4-$CH_3(CH_2)_{15}OC_5H_4N$); cyclam (Cy) - 1,4,8,11-tetraazacyclotetradecane; X - 4-$BrC_6H_4COO^-$.

Complex	Wavenumbers					
	O-H	N-H	CH_2	COO	C-O	C-N
$[Cu(Cy)(H_2O)_2](X)_2.2H_2O$	3373 br	3191 br	-	1549 m (asym) 1379 s (sym)	-	1097 m
$[Cu(Cy)(L)_2](X)_2.2H_2O$	3387 br	3182 br	2917 s (asym) 2851 s (sym)	1638 m (asym) 1472 s (sym)	1189 s	1097 m

Synthesis and chemical structural elucidation of [Cu(Cy)($H_2O)_2$](X)$_2$.2H_2O

The coordination complex [Cu(Cy)($H_2O)_2$](X)$_2$.2H_2O was synthesized through a two-step process. Initially, the copper(II) complex [$Cu_2(X)_4(EtOH)_2$].2H_2O was prepared by a solution-based method. Copper sulfate pentahydrate and potassium 4-chlorobenzoate were dissolved in ethanol and heated for 30 minutes, resulting in the formation of the desired complex.

In the second step of complex synthesis, [$Cu_2(X)_4(EtOH)_2$].2H_2O was reacted with cyclam in ethanol to form a copper-cyclam intermediate. Later, the ligand L (structure shown in Figure 1) was introduced to this intermediate, resulting in the formation of [Cu(Cy)($H_2O)_2$](X)$_2$.2H_2O. The product had a yield of 57.7% and was separated as purple needle-like crystals. Elemental analysis of the complex confirmed its chemical formula as $C_{24}H_{40}CuBr_2N_4O_8$, indicating the presence of copper (Cu), cyclam (a macrocyclic ligand), 4-chlorobenzoate anions, and water molecules of hydration. The calculated and found elemental percentages closely matched Calc.: C, 39.2; H, 5.5; N, 7.6%. Found: C, 39.5; H, 5.7; N, 7.9%, further supporting the proposed formula.

The FTIR spectrum of the compound [Cu(Cy)($H_2O)_2$](4-Br$C_6H_4COO)_2$.2H_2O displayed a broad band at 3342 cm^{-1} due to O-H stretching of water molecules, and another broad band at 3200 cm^{-1} attributed to N-H stretching of the secondary amine group. Additional bands were observed at 1548 cm^{-1} (medium intensity) and 1374 cm^{-1} (strong intensity), corresponding to the asymmetric (ν_{asym}COO) and symmetric (ν_{sym}COO) stretching vibrations of the carboxylate group, respectively. Furthermore, a medium band at 1095 cm^{-1} was indicative of C-N stretching. The calculated ΔCOO value of 170 cm^{-1} is consistent with the presence of non-coordinated 4-Br$C_6H_4COO^-$ ions [33, 34], as confirmed by the crystal structure. The FTIR results are shown in Figure 2.

The UV-Vis spectrum of the compound [Cu(Cy)($H_2O)_2$](X)$_2$.2H_2O in $CHCl_3$ displayed a broad d-d band at 544 nm (ε_{max} = 78.6 M^{-1} cm^{-1}), indicating a trans-III octahedral geometry. This observation is consistent with previous studies on similar complexes [35, 36]. The agreement between the solid-state molecular structure and the solution-phase UV-Vis spectrum suggests that the octahedral geometry is retained in both environments. The UV results are shown in Figure 3a.

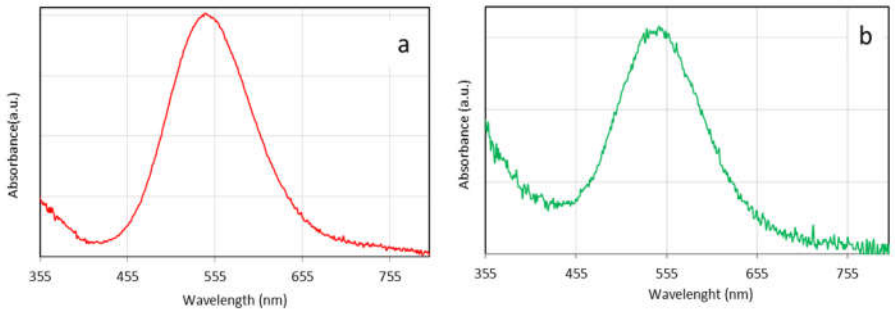

Figure 3. (a) UV-Vis spectrum of [Cu(Cy)($H_2O)_2$](X)$_2$.2H_2O and (b) [Cu(Cy)($L)_2$](X)$_2$.2H_2O.

The magnetic moment (μeff) of the complex [Cu(Cy)($H_2O)_2$](X)$_2$.2H_2O, calculated from the observed magnetic susceptibility data, was found to be 1.9 Bohr magnetons at 298 K. This value (1.80-2.26 B.M.) falls within the expected range for mononuclear patterned copper complex in the distorted octahedral shape geometry [37-41], suggesting that the complex likely adopts a similar structure. The agreement between the experimental μeff value and the theoretical range provides further evidence for the proposed coordination environment of the copper(II) ion in the complex.

Synthesis and structural analysis of [Cu(Cy)(L)$_2$](X)$_2$.2H$_2$O

The reaction of [Cu(Cy)(H$_2$O)$_2$](X)$_2$.2H$_2$O with the ligand L(4-hexadecyl pyridine) yielded the final complex [Cu(Cy)(L)$_2$](X)$_2$. 2H$_2$O. This compound had a yield of 68.5% and was separated as a purple powder. The compound's elemental makeup was found to be as follows: C, 59.2; H, 8.3; N, 6.3%. Found: H: 8.6; N: 6.5%; C: 59.9. These values closely matched the theoretical values calculated from the proposed chemical formula, $C_{66}H_{10}CuBr_2N_6O_6$, which has a molecular weight of 1338.9 g/mol. The FTIR spectrum of the compound [Cu(Cy)(L)$_2$](X)$_2$.2H$_2$O exhibits characteristic peaks indicative of the presence of various functional groups. A broad band at 3359 cm^{-1} confirms the presence of O-H stretching vibrations associated with water molecules. The stretching vibration of N-H in the pyridine part in the ligand L is observed at 3183 cm^{-1}. Additionally, peaks at 2915 cm^{-1} and 2849 cm^{-1} correspond to the asymmetric and symmetric C-H stretching vibrations of methylene groups, respectively. The C=N stretching frequency of the pyridine moiety is evident at 1638 cm^{-1}, while the asymmetric and symmetric C-O stretching vibrations of the carboxylate group appear at 1638 cm^{-1} and 1472 cm^{-1}, respectively. The frequency of stretching of the C-O ether part in the ligand is observed at 1284 cm^{-1}, and the C-N stretching frequency of the cyclam moiety is seen at 1189 cm^{-1}. The calculated ΔCOO value of 166 cm^{-1} suggests that the 4-BrC_6H_4COO- ions are not coordinated to the metal center, as reported in previous studies [38, 39]. The FTIR results are shown in Figure 2.

The UV-Vis spectrum of the complex [Cu(Cy)(L)$_2$](X)$_2$.2H$_2$O displayed a broader d-d absorption band centered to the broad d-d band at 542 nm (ε_{max} = 43.7 M^{-1} cm^{-1}), this suggests a trans-III octahedral shape [40, 41]. This spectral observation aligns with the previously characterized complex [Cu(Cy)(L)$_2$](X)$_2$.2H$_2$O, suggesting that the copper(II) ion in the current complex is also surrounded by a similar octahedral arrangement of ligands. The UV results are shown in Figure 3b.

The magnetic moment (μ_{eff}) of the complex [Cu(Cy)(L)$_2$](X)$_2$.2H$_2$O was calculated at 298 K which is 1.7 B.M., consistent with a mononuclear copper(II) complex in an octahedral shape geometry [42-44]. However, it was lower than the μ_{eff} value of the ligand (L) free complex, [Cu(Cy)(H$_2$O)$_2$](X)$_2$.2H$_2$O (1.9 B.M.), suggesting an influence of the ligand (L). The electron-releasing nature of the alkyl group in L strengthens the N-Cu(II) bonds in axial direction, leading to a less distortion in octahedral geometry and a slightly reduced μ_{eff} value.

Based on the instrumental data analysis and theoretical background the possible structure of the compound is illustrated in the Figure 4.

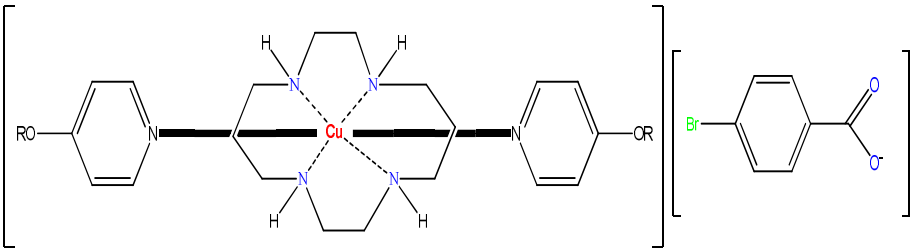

Figure 4. Tentative structure of [Cu(Cy)(L)$_2$](X)$_2$.2H$_2$O. (R = $OC_{16}H_{33}$); lattice H$_2$O are not shown for simplifying the diagram. Where ligand (L); (4-$CH_3(CH_2)_{15}OC_5H_4N$); cyclam (Cy); 1,4,8,11-tetraazacyclotetradecane; X; 4-Br$C_6H_4COO^-$.

Thermal behavior of [Cu(Cy)(H$_2$O)$_2$](X)$_2$.2H$_2$O and [Cu(Cy)(L)$_2$](X)$_2$.2H$_2$O

Thermogravimetric analysis (TGA) of [Cu(Cy)(H$_2$O)$_2$](X)$_2$.2H$_2$O revealed a two-step decomposition pattern which is shown in Figure 5a. The initial weight loss of 6.0% (theoretical:

5.0%) between 74 and 92 °C corresponded to the loss of lattice water molecules. The subsequent major weight loss of 86.1% (theoretical: 86.4%) from 242 °C to 760 °C was attributed to the decomposition of coordinated water, the cyclam ligand, and 4-$BrC_6H_4COO^-$ ions. The final residue of 7.9% (theoretical: 8.6%) at temperatures above 760 °C was consistent with the formation of CuO. These results confirmed the proposed chemical formula and indicated a thermal stability $[Cu(Cy)(H_2O)_2](X)_2.2H_2O$ complexes, with a decomposition temperature of approximately 242 °C.

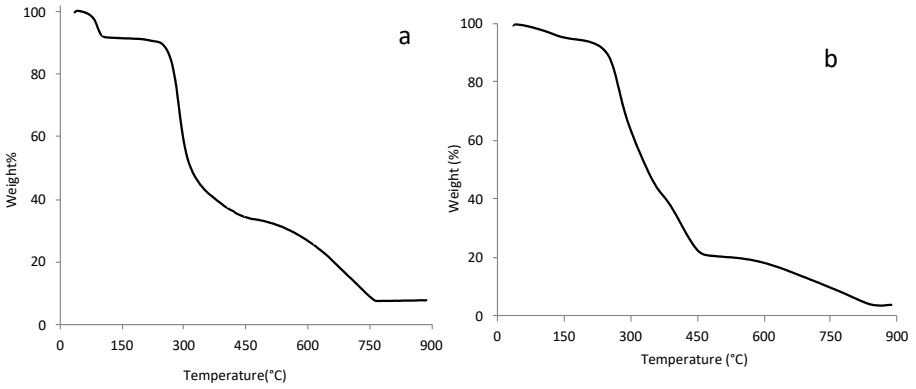

Figure 5. (a) UV-Vis spectrum of $[Cu(Cy)(H_2O)_2](X)_2.2H_2O$ and (b) $[Cu(Cy)(L)_2](X)_2.2H_2O$.

Thermogravimetric analysis (TGA) of the final compound $[Cu(Cy)(L)_2](X)_2.2H_2O$ revealed a two-step decomposition process (Figure 5b). An initial weight loss of 4.0% (theoretical: 2.7%) occurred between 51 and 138 °C, attributed to the loss of lattice water. The subsequent major weight loss of 91.7% (theoretical: 92.6%) from 224 °C to 836 °C corresponded to the decomposition of the cyclam, 4-hexadecyloxypyridine, and 4-$BrC_6H_4COO^-$ ligands. The major weight loss of 86.1% observed in the thermogravimetric analysis (TGA) of the compound $[Cu(Cy)(L)_2](X)_2.2H_2O$ is attributed to the decomposition of coordinated water molecules, the cyclam ligand (Cy), and the 4-bromobenzoate ions. This significant weight loss occurs between 242 °C and 760 °C, indicating the breakdown of the complex's organic and inorganic components. The theoretical weight loss calculated for this decomposition is 86.4%, which closely matches the experimental value of 86.1%. This confirms the proposed chemical formula and the thermal stability of the complex up to 242 °C. The remaining 4.3% residue at temperatures above 836 °C is consistent with the formation of copper(II) oxide (CuO) because, after the decomposition of the organic components (ligands and counterions), the copper(II) ion remains in the form of its oxide. The theoretical residue for CuO formation is 4.7%, which is in good agreement with the experimental value of 4.3%. This residue is expected as CuO is a stable inorganic compound that forms at high temperatures when organic ligands and counterions are completely decomposed. These results confirm the proposed chemical formula of the compound $[Cu(Cy)(L)_2](X)_2.2H_2O$ and indicate a decomposition temperature of 224 °C.

Mesomorphic properties of the complex $[Cu(Cy)(L)_2](X)_2.2H_2O$

Differential scanning calorimetry (DSC) analysis of compound $[Cu(Cy)(L)_2](X)_2.2H_2O$ was conducted over a temperature range of 25-130 °C (Figure 6). There were three different endothermic peaks found during the heating cycle. A transition from crystal to mesophase is represented by the first peak at 42.3 °C ($\Delta H = +38.4$ kJ mol^{-1}), while a transition from mesophase

to mesophase is represented by the second peak at 81.3 °C (ΔH = +19.3 kJ mol^{-1}). Mesophase to isotropic liquid phase transition is shown by the last endothermic peak at 111.7 °C (ΔH = +31.4 kJ mol^{-1}). The isotropic liquid-to-mesophase transition was represented by a single exothermic peak in the differential scanning calorimetry (DSC) analysis because this transition involves the release of energy as the compound transitions from a disordered isotropic liquid state to a more ordered mesophase. The exothermic peak at 72.7 °C (ΔH = -2.2 kJ mol^{-1}) indicates that the system is losing energy as it reorganizes into a liquid crystalline phase. This is a typical behavior for liquid crystalline materials, where the transition from an isotropic liquid to a mesophase is exothermic due to the increase in molecular order. At 42 °C, the compound $[Cu(Cy)(L)_2](X)_2.2H_2O$ undergoes a crystal-to-mesophase transition, which corresponds to the melting of the crystalline solid into a liquid crystalline phase. This transition is endothermic, as indicated by the DSC peak at 42.3 °C (ΔH = +38.4 kJ mol^{-1}). At 111°C, the compound transitions from the mesophase to an isotropic liquid phase, which is also an endothermic process (ΔH = +31.4 kJ mol^{-1}). This transition occurs because, at higher temperatures, the thermal energy overcomes the intermolecular forces that maintain the ordered mesophase, resulting in a disordered isotropic liquid. These transitions are characteristic of liquid crystalline materials, which exhibit multiple phase changes with increasing temperature. The long-chain pyridine ligand (4-hexadecyloxypyridine) plays a crucial role in influencing the mesophase formation and stability. The extended alkyl chain enhances the molecular flexibility and promotes self-assembly, leading to the formation of stable mesophases. The presence of the pyridine ring further facilitates coordination with the Cu(II) center, stabilizing the complex's liquid crystalline behavior. This structural arrangement is critical in enhancing the thermal stability and contributing to the distinct phase transitions observed in DSC and POM analyses.

The magnetic moment of 1.7 B.M. at room temperature suggests a mononuclear Cu(II) complex with an octahedral geometry. This value aligns with the expected range for Cu(II) complexes, where the unpaired electron in the d-orbital contributes to the magnetic behavior. The coordination environment created by the cyclam ligand and the 4-bromobenzoate counterion further stabilizes the electronic structure, leading to the observed magnetic properties. The slight reduction in the magnetic moment compared to the free Cu(II) ion can be attributed to ligand field effects and spin-orbit coupling. The DSC results reveal distinct phase transitions, including the crystal-to-mesophase transition at 42.3 °C, mesophase-to-mesophase transition at 81.3 °C, and mesophase-to-isotropic transition at 111.7 °C. These transitions are consistent with those observed in similar copper-based metallomesogens, confirming the thermal stability of the complex.

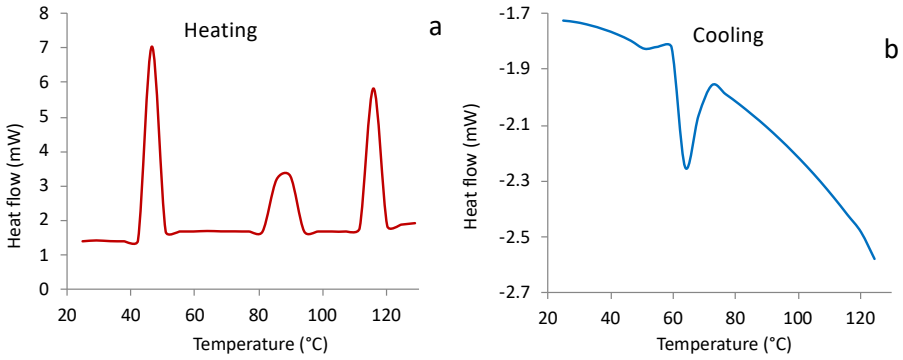

Figure 6. Liquid crystallinity evaluation of $[Cu(Cy)(L)_2](X)_2.2H_2O$ by DSC (a) DSC scans in the temperature range of 25 to 130 °C for (a) heating and (b) cooling.

The POM analysis further supports these findings, showing characteristic optical textures upon cooling, indicative of the formation of stable liquid crystalline phases. The compound exhibited a thermal phase change under polarized optical microscopy (POM). At 42 °C, it melted, and at 111 °C, it changed into an isotropic liquid phase. A distinctive liquid crystalline phase was seen at 78.0 °C after cooling from the isotropic liquid phase, as shown in Figure 7. This observation confirms the mesogenic nature of the compound. The lower transition temperatures compared to other metallomesogens suggest that the long alkyl chain and the cyclam coordination environment effectively lower the energy barrier for phase transitions, making this complex suitable for applications in advanced display technologies and molecular electronics. These insights demonstrate the significant influence of molecular structure on the mesomorphic and magnetic behavior of the complex, providing a foundation for future design and optimization of metallomesogens for specific applications in functional materials.

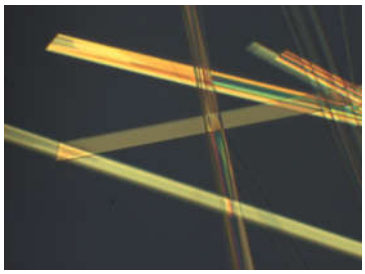

Figure 7. Liquid crystallinity evaluation of $[Cu(Cy)(L)_2](X)_2.2H_2O$ by POM photomicrographs on cooling of the compound at 77.3 °C.

Comparison of thermal stability and liquid crystalline phases with other metallomesogens

To demonstrate the superiority of our synthesized Cu(II) complex, a comparative analysis with previously reported metallomesogens and Cu(II)-based materials is provided.

Electrochemical performance. The redox behavior of Cu(II) in $[Cu(Cy)(L)_2](X)_2.2H_2O$ liquid was analyzed and compared with other metallomesogens reported in the literature. Our findings suggest that the presence of the cyclam ligand stabilizes the Cu(II) center, resulting in enhanced electrochemical reversibility and higher charge transport efficiency. Similar Cu(II) complexes have been explored in the context of electrochemical sensors and catalysis, but our system demonstrates superior redox stability due to the macrocyclic coordination environment.

Structural influence. Unlike open-chain ligand-based Cu(II) complexes, the incorporation of the cyclam ligand in our system leads to a more rigid coordination sphere, reducing structural distortion and improving electronic properties.

Thermal and mesomorphic stability. Our compound exhibited a higher decomposition temperature (224 °C) compared to other reported metallomesogens, which enhances its potential for applications in optoelectronic devices.

Mechanistic insights. The presence of the long-chain pyridine ligand facilitates the formation of columnar mesophases, crucial for anisotropic electronic conduction, making it a suitable candidate for organic electronic applications.

CONCLUSION

This study successfully synthesized and characterized a novel Cu(II)-based metallomesogen, $[Cu(Cy)(H_2O)_2](X)_2.2H_2O$ demonstrating liquid crystalline and electrochemical properties. The complex exhibited well-defined mesophases, confirmed by DSC and POM analysis, with phase transitions indicative of stable liquid crystal behavior. The incorporation of the cyclam ligand and 4-hexadecyloxypyridine enhanced both mesomorphic and magnetic properties, making this material promising for display technologies, molecular electronics, and optical devices**.** Future research should focus on modifying ligand structures to fine-tune mesophase stability and optimize electrochemical behavior. The integration of additional metal centers could enhance functional properties, paving the way for applications in organic light-emitting diodes (OLEDs), flexible displays, and smart sensors**.** Additionally, exploring these materials for energy storage applications, catalysis, and electrochemical sensing could unlock new possibilities. The scalability of this synthesis should also be examined to facilitate industrial applications**.** Further studies on thin-film fabrication and electronic conductivity measurements could expand the scope of these metallomesogens in next-generation devices. This research provides a foundation for developing multi-functional materials with potential applications in both optoelectronic and energy-related technologies, bridging the gap between fundamental chemistry and practical innovations.

ACKNOWLEDGMENTS

Naima Sharmin would like to express my sincere gratitude to my esteemed doctoral advisor, Assoc. Prof. Dr. Norbani Abdullah, from the Department of Chemistry, University of Malaya. This research was generously supported by the University of Malaya through research grants FP008/2011A, PV056/2012A, and UM.C/625/1/HIR/MOHE/CHAN/05. Furthermore, Naima Sharmin would like to extend her heartfelt thanks to all the dedicated staff members of the Department of Chemistry, University of Malaya. The authors extend their appreciation to Taif University, Saudi Arabia, for supporting this work through project number (TU-DSPP-2024-06).

REFERENCES

1. Hayami, S.; Kojima, Y.; Urakami, D.; Ohta, K.; Inoue, K. Mesophase and magnetic behavior in cobalt(II) and iron(II) compounds. *Polyhedron* **2009**, 28, 2053-2057.
2. Klaus G.; Athanassopoulou, M.A.; Bustamante, E.S.; Haase, W.; Zbigniew, T.; Zaleski, A.J. A ferrimagnetically coupled liquid crystal. *Adv. Mater*. **1997**, 9, 45-48.
3. Bałanda, M.; Falk, K.; Griesar, K.; Tomkowicz, Z.; Wasiutyński, T.; Haase, W. Spin Flop transition in the substituted Mn-porphyrin magnet $[Mn(OC_{12}H_{25})_4TPP][TCNE]$* 2PhMe. *Mol. Cryst. Liq. Cryst. Sci. Technol. Sect. A Mol. Crys. Liq. Cryst*. **1999**, 335, 133-141.
4. Kirsch, P.; Bremer, M. Nematic liquid crystals for active matrix displays: Molecular design and synthesis. *Angew. Chem. Int. Ed.* **2000**, 39, 4216-4235.
5. Yang, D.K.; Wu, S.T. *Fundamentals of liquid crystal devices*. John Wiley & Sons; **2014**.
6. Cuerva, C.; Cano, M.; Lodeiro, C. Advanced functional luminescent metallomesogens: The Key role of the metal center. *Chem. Rev.* **2021**, 121, 12966-13010.
7. Damm, C.; Israel, G.; Hegmann, T.; Tschierske, C. Luminescence and photoconductivity in mononuclear ortho-platinated metallomesogens. *J. Mat. Chem.* **2006**, 16, 1808-1808.
8. Seredyuk, M. Iron(II) metallomesogens based on symmetrical tripod ligands. *Inorg. Chim. Acta* **2011**, 380, 65-71.
9. Blake, A.B.; Sinn, E.; Yavari, A.; Moubaraki, B.; Murray, K.S. Magnetic properties of binuclear manganese(II), cobalt(II), nickel(II) and copper(II) complexes of a macrocyclic

ligand derived from pyridine-N-oxide, and crystal structure of the nickel complex. *Inorg. Chim. Acta* **1995**, 229, 281-290.
10. Butcher, R.J.; Overman, J.W.; Sinn, E. Bi- and polynuclear antiferromagnetic metal complexes (copper, nickel) with salicylaldimines and acetate-type ligands. New modes of acetate bridging. *J. Am. Chem. Soc.* **1980**, 102, 3276-3278.
11. Sinn, E. in: Townshend, A. (Ed.). *Encyclopaedia of Analytical Chemistry*, Academic Press: Online Publication; **1995**, pp. 2765-2780.
12. Giroud-Godquin, A.M.; Maitlis, P.M. Metallomesogens: Metal complexes in organized fluid phases. *Angew. Chem.* **1991**, 30, 375-402.
13. Bruce, D.W. in: Bruce, D.W.; O'Hare, D. (Eds.). *Inorg. Mat.*, 2nd ed., Wiley: New York; **1996**, 429-522.
14. Cukiernik, F.D.; Ibn-Elhaj, M.; Chaia, Z.D.; Marchon, J.-C.; Giroud-Godquin, A.-M.; Guillon, D.; Skoulios, A.; Maldivi, P. Mixed-valent diruthenium (II, III) long-chain carboxylates. 1. Molecular design of columnar liquid-crystalline order. *Chem. Mat.* **1998**, 10, 83-91.
15. Kang, S.J.; Ahn, S.; Kim, J.B.; Schenck, C.; Hiszpanski, A.M.; Oh, S.; Schiros, T.; Loo, Y.-L.; Nuckolls, C. Using self-organization to control morphology in molecular photovoltaics. *J. Am. Chem. Soc.* **2013**, 135, 2207-2212.
16. Dalcanale, E. in: Atwood, J.L.; Davies, J. E. D.; MacNicol, D. D.; Vogtle, F. (Eds.). *Comp. Supramol. Chem.* **1996**, 10, 583-635.
17. Boden, N.; Bissell, R.; Clements, J.; Movaghar, B. Discotic liquid crystals. *Liq. Cry. Today*. **1996**, 6, 1-4.
18. Simmerer, J.; Glüsen, B.; Paulus, W.; Kettner, A.; Schuhmacher, P.; Adam, D.; Karl-Heinz E.; Siemensmeyer, K.; Wendorff, J.H.; Helmut, R.; Haarer, D. Transient photoconductivity in a discotic hexagonal plastic crystal. *Adv. Mat.* **1996**, 8, 815-819.
19. Osburn, E.J.; Schmidt, A.; Chau, L.-K.; Chen, S.-Y.; Smolenyak, P.; Armstrong, N.R.; O'Brien, D.F. Supramolecular fibers from a liquid crystalline octa-substituted copper phthalocyanine. *Adv. Mat.* **1996**, 8, 926-928.
20. Van Nostrum, C.F.; Nolte, R.J.M. Functional supramolecular materials: Self-assembly of phthalocyanines and porphyrazines. *Chem. Comm.* **1996**, 21, 2385-2392.
21. Wendorff, J.H.; Christ, T.; Glüsen, B.; Greiner, A.; Kettner, A.; Sander, R.; Stümpflen, V.; Tsukruk, V.V. Columnar discotics for light emitting diodes. *Adv. Mat.* **1997**, 9, 48-52.
22. Liu, C.Y.; Pan, H.L.; Fox, M.A.; Bard, A.J. High-density nanosecond charge trapping in thin films of the photoconductor ZnODEP. *Sci.* **1993**, 261, 897-899.
23. Schmidt, S.; Lattermann, G.; Kleppinger, R.; Wendorff, J.H. Octahedral metallo-mesogens of chromium, molybdenum and tungsten with 1,4,7-trisubstituted 1,4,7-triazacyclononane and three carbonyl groups as ligands. *Liq. Cryst.* **1994**, 16, 693-702.
24. Bryant, G.C.; Cook, M.J.; Haslam, S.O.; Richardson, R.M.; Ryan, T.G.; Thorne, A.J. Discotic liquid-crystal behaviour of some multinuclear phthalocyanine derivatives. *J. Mat. Chem.* **1994**, 4, 209-209.
25. Doppelt, P.; Huille, S. Mesogenic Octakis (octylthio) tetraazametalloporphyrins. *New J. Chem*. **1990**, 14, 607-609.
26. Liebmann, A.; Mertesdorf, C.; Plesnivy, T.; Ringsdorf, H.; Wendorff, J.H. Complexation of transition metal ions with substituted aza macrocycles: Induction of columnar mesophases by molecular recognition. *Angew. Chem. Int. Ed.***1991**, 30, 1375-1377.
27. Lelievre, D.; Bosio, L.; Simon, J.; Andre, J.J.; Bensebaa, F. Dimeric substituted copper phthalocyanine liquid crystals. Synthesis, characterization and magnetic properties. *J. Am. Chem. Soc.* **1992**, 114, 4475-4479.
28. Wu, H.-C.; Sung, J.-H.; Yang, C.-D.; Lai, C.K. Ionic hexagonal columnar metallomesogens derived from tetrabenzo[*b,f,j,n*] [1,5,9,13]tetraazacyclohexadecine. *Liq. Cryst.* **2001**, 28, 411-415.

29. Neumann, B.; Hegmann, T.; Tschierske, C.; Neumann, B.; Wolf, R. Binuclear cyclopalladated cyclophanes: Towards a new family of metallomesogens. *Chem. Commun.* **1998**, 1, 105-106.
30. Janeczek, H.; Duale, K.; Sikorska, W.; Godzierz, M.; Kordyka, A.; Marcinkowski, A.; Rydz, J. Poly (L-lactide) liquid crystals with tailor-made properties toward a specific nematic mesophase texture. *ACS Sustain. Chem. Eng.* **2022**, 10, 3323-3334.
31. Abdullah, N.; Sharmin, N.; Ozair, L.N.; Nordin, A.R.; Siti, W.; Mohamadin, M.I. Structures and mesomorphism of complexes of tetrakis(4-chlorobenzoate-μ-O,O′)bis(ethanol) dicopper(II) with different N-donor ligands. *J. Coord. Chem.* **2015**, 68, 1347-1360.
32. Bain, G.A.; Berry, J.F. Diamagnetic corrections and Pascal's constants. *J. Chem. Educ.* **2008**, 85, 532.
33. Burrows, H.D.; Ellis, H.A. The thermal behaviour and spectral properties of some long chain copper(II) carboxylates. *Thermochim. Acta* **2001**, 52, 121-129.
34. Cabaniss, S.E.; McVey, I.F. Aqueous infrared carboxylate absorbances: Aliphatic monocarboxylates. *Spectrochim. Acta Part A* **1995**, 51, 2385-2395.
35. Bucher, C.; Duval, E.; Barbe, J.-M.; Verpeaux, J.-N.; Amatore, C.; Guilard, R. Synthesis, characterization and X-ray crystal structure of cyclam derivatives. Part III. Formation and electrochemically induced isomerization of copper complexes of 1,8-bis(N,N-dimethylcarbamoylmethyl)-4,11-dimethyl-1,4,8,11-tetraazacyclotetradecane. *Compt. Rend. de l'Acad. Des Sci. - Series IIC – Chem.* **2000**, 3, 211-222.
36. Chapman, J.; Ferguson, G.; Gallagher, J. F.; Jennings, M.C.; Parker, D. Copper and nickel complexes of 1,8-disubstituted derivatives of 1,4,8,11-tetraazacyclotetradecane. *J. Chem. Soc. Dalton Trans.* **1992**, 3, 345-345.
37. Kahn, O. *Molecular Magnetism*. VCH-Verlag: Weinheim; **1993**.
38. Cristóvão, B. Spectral, thermal and magnetic properties of Cu(II) and Ni(II) complexes with Schiff base ligands. *J. Ser. Chem. Soc.* **2011**, 76, 1639-1648.
39. Busch, D.H.; Katović, V.; Taylor, L.T. Nickel(II) and copper(II) complexes containing new monocyclic and polycyclic ligands derived from the cyclotetrameric Schiff base of o-aminobenzaldehyde. *Inorg. Chem.* **1971**, 10, 458-462.
40. Boudreaux, E.A. Theoretical study of the magnetic moments of Cu(II) complexes. Part 1.—Symmetrical trigonal bipyramidal and square pyramidal co-ordination. *Trans. Faraday Soc.* **1963**, 59, 1055-1058.
41. Sacconi, L.; Ciampolini, M.; Campigli, U. Magnetic investigation of some tetracoordinated nickel(II) and copper(II) complexes between 80 and 300 K. *Inorg. Chem.* **1965**, 4, 407-409.
42. Pajtášová, M.; Ondrušová, D.; Jóna, E.; Mojumdar, S.C.; L'alíková, S.; Bazyláková, T.; Gregor, M. Spectral and thermal characteristics of copper(II) carboxylates with fatty acid chains and their benzothiazole adducts. *J. Therm. Anal. Calorim.* **2010**, 100, 769-777.
43. Badea, M.; Emandi, A.; Marinescu, D.; Cristurean, E.; Olar, R.; Braileanu, A.; Budrugeac, P.; Segal, E. *J. Therm. Anal. Calorim.* **2003**, 72, 525-531.
44. Joseyphus, S.; Sivasankaran, R.; Nair, M. Synthesis, characterization and biological studies of some Co(II), Ni(II) and Cu(II) complexes derived from indole-3-carboxaldehyde and glycylglycine as Schiff base ligand. *Arab. J. Chem.* **2010**, 3, 195-204.